

# Nb rich precipitates in Inconel 718 produced by selective laser melting

R. V. Shakhov<sup>1,†</sup>, K. Sh. Mukhtarova<sup>2</sup>

<sup>†</sup>shakhov-rv@yandex.ru

<sup>1</sup>Institute for Metals Superplasticity Problems of RAS, 39 Khalturin st., Ufa, 450001, Russia

<sup>2</sup>Ufa State Aviation Technical University, 12 Karl Marx st., Ufa, 450008, Russia

Microstructure of nickel-based superalloy Inconel 718 produced by selective laser melting (SLM) was studied by electron microscopy. Multiple cycles of heating and rapid cooling during SLM lead to the formation of a complex microheterogeneous structure in the alloy. At the same time, a chemical analysis of such a microstructure showed a high homogeneity. The microstructure consisted of  $\gamma$  grains with a size of about 10  $\mu\text{m}$  banded with  $\delta$  phase particles and small carbides. Scanning and transmission electron microscopy examination showed that the  $\gamma$  grains consisted of columnar and equiaxed subgrains. The intermetallic phases based on  $\text{Ni}_3\text{Nb}$  ( $\gamma''$  and  $\delta$ ) were found to be homogeneously precipitated. The volume fraction of these precipitates was experimentally defined to be about 20%. The carbides with dimensions of 2 – 10  $\mu\text{m}$  typically observed in Inconel 718 manufactured by conventional ingot metallurgy were not detected. The untypical microstructure of the SLM material presumably resulted from fast cooling during SLM process. The maximum volume fraction of the intermetallic phases  $\gamma''$  and  $\delta$  was also calculated on the assumption that niobium was not dissolved in the matrix  $\gamma$  phase. The calculated volume fraction of the niobium containing phases was determined to be 13.6%. Energy dispersive X-Ray analysis of niobium containing precipitates showed that the  $\text{Ni}_3\text{Nb}$  based intermetallic phases also contained molybdenum and titanium. The maximum volume fractions of virtual intermetallic phases  $\text{Ni}_3\text{Ti}$  and  $\text{Ni}_3\text{Mo}$  were calculated on the assumption that these elements were not dissolved in the matrix  $\gamma$  phase as well. The calculated volume fractions of these virtual phases were shown to be equal to 4.3 and 7.5%, correspondingly. The defined volume fraction of niobium containing phases was less than the calculated volume fraction (20% against 25.4%). This suggests that Nb, Ti and Mo were not completely presented in the niobium containing phases and were partially dissolved in the matrix  $\gamma$  phase during SLM process.

**Keywords:** nickel-based superalloy, intermetallic phase, microstructure, selective laser melting.

УДК: 669-1

## Нб-содержащие выделения сплава Inconel 718 изготовленного селективным лазерным плавлением

Шахов Р. В.<sup>1,†</sup>, Мухтарова К. Ш.<sup>2</sup>

<sup>1</sup>Институт проблем сверхпластичности металлов РАН, ул. Ст. Халтурина, 39, Уфа, 450001, Россия

<sup>2</sup>Уфимский государственный авиационный технический университет, ул. К. Маркса, 12, Уфа, 450008, Россия

Исследование микроструктуры никелевого сплава Inconel 718, изготовленного методом селективного лазерного плавления (SLM), проводилось с помощью электронной микроскопии. Множественные циклы нагрева и быстрого охлаждения во время его производства привели к образованию сложной микрогетерогенной структуры. В то же время химический анализ такой микроструктуры показал высокую однородность. Микроструктура состоит из зерен размером около 15  $\mu\text{m}$ , по границам которых выделены частицы  $\delta$  фазы и небольшие карбиды. Электронно-микроскопические исследования показали, что столбчатые субзерна состоят из равноосных субзерен размером около 0,5  $\mu\text{m}$ . Показано, что интерметаллидные фазы на основе  $\text{Ni}_3\text{Nb}$  ( $\gamma''$  и  $\delta$ ) выделяются гомогенно. Объемная доля этих выделений была экспериментально определена и составила около 20%. Карбиды с размерами 2 – 10  $\mu\text{m}$ , обычно наблюдаемые в промышленных горячекованных сплава Inconel 718, не были обнаружены. Необычная микроструктура SLM сплава, по-видимому, была обусловлена быстрым охлаждением в процессе его изготовления и высокой химической однородностью исходного порошка. Максимальная объемная доля интерметаллидных фаз  $\gamma''$  и  $\delta$  также была теоретически рассчитана в предположении, что ниобий не растворялся в матричной  $\gamma$  фазе. Рассчитанная объемная доля фаз, содержащих ниобий, составила 13,61%. Энергодисперсионный рентгеновский (EDX) анализ выделений показал, что интерметаллидные фазы на основе  $\text{Ni}_3\text{Nb}$  также содержат молибден и титан. Максимальные объемные доли виртуальных интерметаллидных фаз  $\text{Ni}_3\text{Ti}$  и  $\text{Ni}_3\text{Mo}$  были рассчитаны в предположении, что эти элементы не были растворены в матричной  $\gamma$  фазе. Рассчитанные объемные доли этих виртуальных фаз составили, соответственно, 4,34 и 7,49%. Экспериментально определенная объемная доля фаз, содержащих ниобий, была близка к расчетной объемной доле, предполагая, что растворение Mo, Ti в фазах  $\text{Ni}_3\text{Nb}$  и Nb в матричной фазе произошло в некоторой степени во время SLM процесса.

**Ключевые слова:** жаропрочный сплав, Inconel 718, структура сплава,  $\text{Ni}_3\text{Nb}$ , селективное лазерное плавление.

## 1. Introduction

INCONEL 718 is an austenitic nickel-chromium-based superalloy capable of withstanding high mechanical and thermal loads and widely used for rocket and aircraft engine applications [1]. This alloy was used for the production of about 1500 individual parts of Space Shuttle main engine including a combustion chamber. This is more than 50% of the engine mass with a total weight of about 1 ton [2, 3]. The performance characteristics of this alloy depend not only on the chemical but also on the phase composition, as well as on the technology of its production and heat treatment. For example, the use of modern technology of selective laser melting (SLM) is ideally suited for producing components with complex geometries. This process involves multiple cycles of heating and rapid cooling that leads to the formation of a complex microheterogeneous structure with the precipitation of dispersed phases. The precipitated phases, which are the main components responsible for hardening of the alloy, were identified in the work [4]. These include the intermetallic phases:  $DO_{22}$  — ordered  $Ni_3Nb$  ( $\gamma''$ ),  $L1_2$  — ordered  $Ni_3(Al, Ti)$  ( $\gamma'$ ) and  $DO_a$  — ordered  $Ni_3Nb$  ( $\delta$ ). Carbides of the type MC,  $M_6C$ ,  $M_{23}C_6$  and the Laves phase of type  $(Ni, Cr, Fe)_2(Nb, Mo, Ti)$  also can be presented in the microstructure of the alloy [5, 6, 7]. The composition and microstructure of Alloy 718 was studied by STEM X-ray energy dispersive spectrometry in ref. [8]. The main strengthening phase of this alloy is the metastable  $\gamma''$  phase, which can be transformed into the stable  $\delta$  phase [9]. These phases contain Nb and therefore the amount of the strengthening phases and mechanical properties of the alloy depend on the quantity of Nb in intermetallic phases. Basing on this, it is of interest to study microstructure features of SLM alloy and the chemical composition of the niobium containing phases as well as the maximum volume fraction of the  $Ni_3Nb$  based phases in the alloy on an assumption that niobium can be replaced by other alloying elements.

## 2. Experimental procedures

The chemical composition of nickel-based superalloy Inconel 718 produced by SLM in weight percent was taken from ref. [10]. The recalculated chemical composition of the alloy in atomic percent is given in Table 1.

Scanning electron microscopy (SEM) and electron backscattered diffraction (EBSD) analyses were performed by Tescan Vega 3SBH and Mira-3, transmission electron microscopy (TEM) was carried out on a JEOL JEM-2000EX microscope. The samples and foils were polished by Tenupol-5 at 50V using the following electrolyte: 10% perchloric acid + 90% butanol. The chemical composition was determined by SEM equipped with energy dispersive X-Ray (EDX)

system produced by Oxford instruments. The average grain and subgrain sizes as well as the phase composition were determined using TEM and SEM images. EBSD analysis was performed with a scanning step 0.4  $\mu m$  and Ni was chosen as the input phase due to high dispersion of  $\gamma'$ -phase.

Calculations in the present work were done in an assumption that Nb, Ti and Mo entered completely into the composition of the intermetallic phases  $Ni_3(Nb, Ti, Mo)$ . The mass of  $i$ -th element in one mole of the alloy is equal to:

$$m_i = m_{ati} \times at_i, \quad (1)$$

where  $m_{ati}$  is the atomic mass and  $at_i$  the fraction of atoms of  $i$ -th element in the alloy according to Table 1. The mass of phase  $Ni_3Me$  ( $Me = Nb, Mo, Ti$ ) in one mole of the alloy is defined as:

$$M_{Ni_3Me} = m_{atMe} \times at_{Me} + 3m_{atNi} \times at_{Ni}, \quad (2)$$

where  $m_{atMe}$ ,  $m_{atNi}$  and  $at_{Me}$ ,  $at_{Ni}$  are the atomic masses and fractions of Me and Ni, respectively. The mass of one mole of the alloy is calculated by summing the masses of all elements in the alloy:

$$M = \sum m_i. \quad (3)$$

The molar volume of the alloy  $V_{alloy}$  can be determined by dividing its mass by the density  $\rho_{alloy}$ :

$$V_{alloy} = M / \rho_{alloy}. \quad (4)$$

Similarly, volumes of the phase  $Ni_3Me$  in one mole of the alloy is determined as

$$V_{Ni_3Me} = M_{Ni_3Me} / \rho_{Ni_3Me}. \quad (5)$$

Then, the volume fraction of the  $Ni_3Me$  phase in the alloy,  $\varphi_{Ni_3Me}$ , is calculated by the following equation:

$$\varphi_{Ni_3Me} = (V_{Ni_3Me} / V_{alloy}) \times 100\%. \quad (6)$$

## 3. Results and discussion

### 3.1. Microstructure characterization of Inconel 718 obtained by SLM

Fig. 1 represents SEM images of the as-received alloy produced by SLM. The microstructure of alloy consists of  $\gamma$  grains with a size of about 10  $\mu m$ , that correspond to ref. [11], banded with  $\delta$  phase particles and small carbides. The  $\gamma$  grains consist of columnar and equiaxed subgrains (Fig. 1). Nearly the same microstructure was interpreted as cellular and dendritic microstructure [12, 13] observed in columnar grains [14, 15, 16]. SEM and TEM examination showed that the columnar subgrains in their turn consisted of equiaxed subgrains with a size of about 0.5  $\mu m$  (Figs. 1c, 2)

**Table 1.** Chemical composition of Alloy 718.

Cr	Al	Ti	Fe	Nb	Mo	Co	B	C	Ni	%
19	0.5	0.9	18.5	5.1	3	0.1	0.025	0.04	52.8	wt.
21.15	1.072	1.08	19.17	3.18	1.81	0.098	0.134	0.192	52.09	at.

[7, 17]. The  $\delta$ -phase plates were mainly located along grain boundaries [7, 18] as it takes place in the commercial alloy Inconel 718 [2, 4] (Fig. 1).

Dispersed  $\gamma''$  particles with a size less than 50 nm were homogeneously precipitated during cooling (Fig. 2). Interestingly, carbides with a size of 2–10  $\mu\text{m}$  typically observed in this commercial alloy were not detected. Thus, the use of SLM resulted in a very untypical microstructure in Inconel 718. The microstructure features of the SLM material include a developed substructure in  $\gamma$  grains and the presence of dispersed precipitates along subgrain boundaries.

Fig. 3 illustrates the distribution of Nb, Mo and Ti in the SLM material. EDX analysis showed that Nb, Mo and Ti were homogeneously distributed both in the  $\gamma''$  and  $\delta$  phases. The volume fraction of  $\gamma''$  and  $\delta$  phases was defined using TEM images. The evaluation revealed about 20 vol. % of niobium containing phases. The EDX analysis showed that Nb, Mo and Ti were present in the dispersed  $\gamma''$  and  $\delta$  phase precipitates. It is qualitatively seen that large precipitates of the  $\delta$  phase along with Nb contained also Mo and small quantity of Ti.

From EBSD analysis the grain size and the crystallographic texture of SLM alloy can be determined. Fig. 4 displays microstructure with grain size of about 10  $\mu\text{m}$  that is consistent with the data of SEM micrographs. The fraction

of high-angle grain boundaries on the selected sample area was about 26%.

It is of interest to know the maximum volume fraction of the  $\text{Ni}_3\text{Nb}$  based phases in the alloy on the assumption that niobium may be replaced by Mo and Ti.

### 3.2. Calculation of the volume fractions of the virtual phases

In order to evaluate the maximum amount of the niobium containing hardening phases, volume fractions of virtual phases  $\text{Ni}_3\text{Nb}$ ,  $\text{Ni}_3\text{Mo}$  and  $\text{Ni}_3\text{Ti}$  were calculated basing on the alloy composition given by Table 1 and Eqs. 1–6. For Nb, the atomic mass is equal to 92.9 g/mol and for Ni 58.69 g/mol, and the mass of  $\text{Ni}_3\text{Nb}$  in one mole alloy is  $M_{\text{Ni}_3\text{Nb}} = 0.0318 \times 92.9 + 0.0318 \times 3 \times 58.69 = 8.553$  g. The mass of one mole of the alloy is equal to  $M = 57.885$  g.

Taking for the densities of Inconel 718 alloy and  $\text{Ni}_3\text{Nb}$  phase the values  $\rho_{\text{alloy}} = 8.2$  g/cm<sup>3</sup> [10] and  $\rho_{\text{Ni}_3\text{Nb}} = 8.9$  g/cm<sup>3</sup>, the volume of the  $\text{Ni}_3\text{Nb}$  phase in one mole alloy is estimated to be  $V_{\text{Ni}_3\text{Nb}} = 8.553/8.9 = 0.961$  (cm<sup>3</sup>). The molar volume of the alloy  $V_{\text{alloy}} = 57.885/8.2 = 7.059$  (cm<sup>3</sup>). Then, the maximum volume fraction of the  $\text{Ni}_3\text{Nb}$  phase in the alloy,  $\varphi_{\text{Ni}_3\text{Nb}}$ , defined by Eq. 6 is equal to  $\varphi_{\text{Ni}_3\text{Nb}} = 0.961/7.059 \times 100\% = 13.6\%$ .

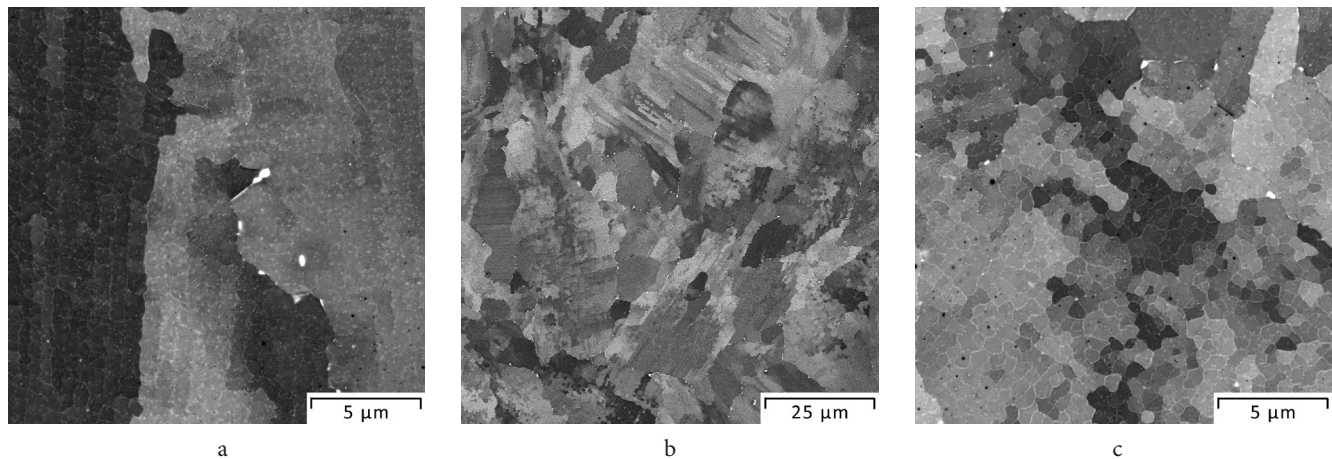


Fig. 1. BSE images of the alloy Inconel 718 obtained by SLM.

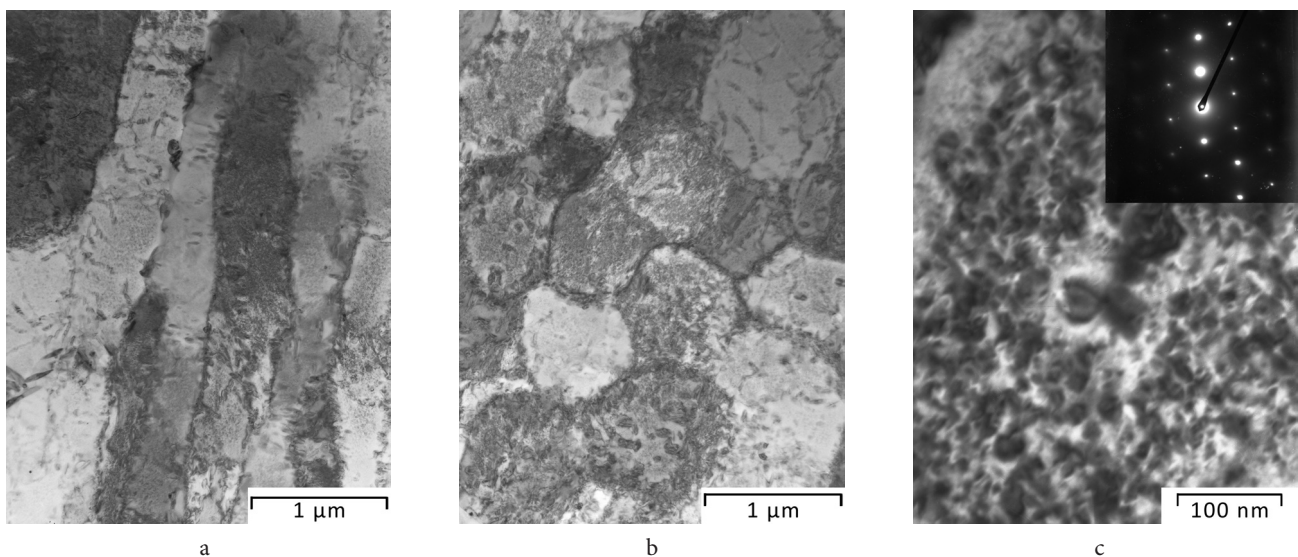
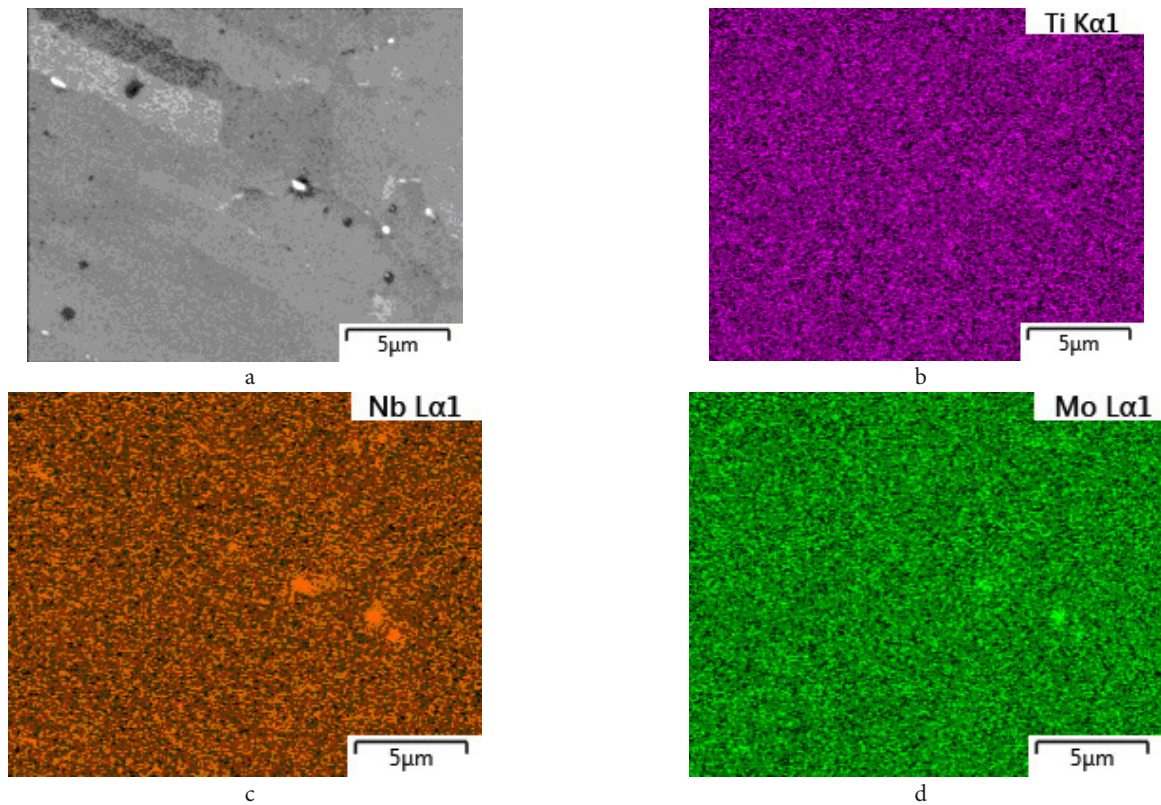
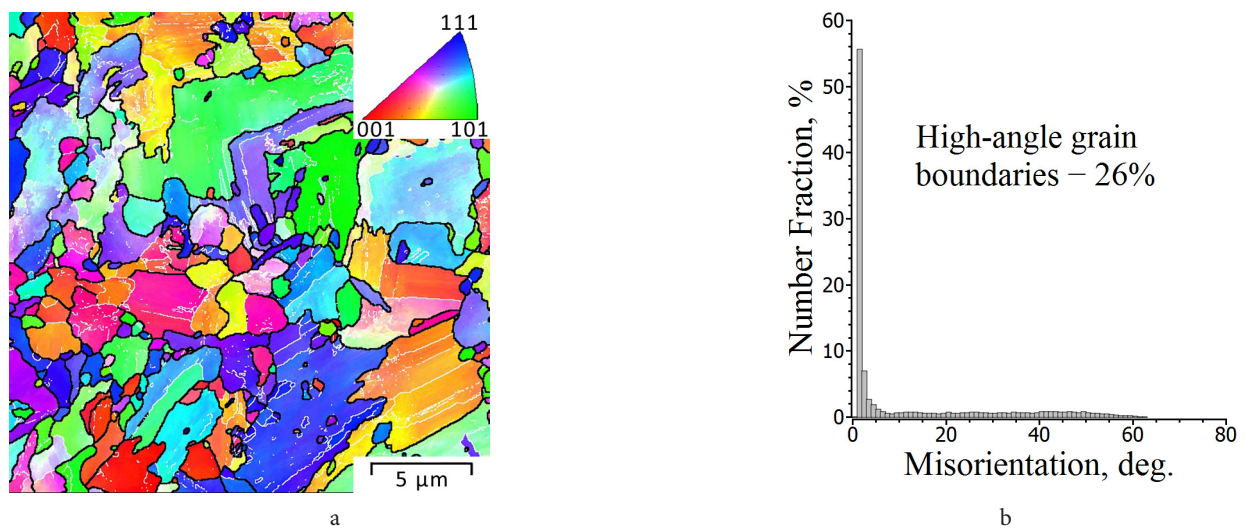


Fig. 2. Bright field TEM images of the alloy Inconel 718 obtained by SLM.



**Fig. 3.** Distribution of Nb, Ti and Mo in the alloy Inconel 718 obtained by SLM.



**Fig. 4.** EBSD orientation map (a) and grain boundary distribution (b) of SLM Inconel 718.

Taking the densities of  $\text{Ni}_3\text{Ti}$  and  $\text{Ni}_3\text{Mo}$  phases 7.9 and 7.9  $\text{g}/\text{cm}^3$ , respectively, similar calculations yield for virtual  $\text{Ni}_3\text{Ti}$  and  $\text{Ni}_3\text{Mo}$  phases the values  $\varphi_{\text{Ni}_3\text{Ti}} = 4.3\%$  and  $\varphi_{\text{Ni}_3\text{Mo}} = 7.5\%$ .

Thus, the maximum volume fraction of  $\text{Ni}_3\text{Nb}$  and virtual  $\text{Ni}_3\text{Ti}$ ,  $\text{Ni}_3\text{Mo}$  phases in the alloy is 25.4%.

The presented calculation is inconsistent with the experimentally defined volume fraction of the niobium containing phases. This discrepancy may be due to the fact that Nb, Ti and Mo were not completely presented in the niobium containing phases and were partially dissolved in the matrix  $\gamma$  phase owing to rapid cooling and slow diffusion during SLM process. Note that the calculated volume fraction of niobium containing phases (25.4%) is close to the

experimentally defined volume fraction of these phases in ref. [19]. Probably, a higher quantity of the niobium containing phases was precipitated during annealing. The authors in ref. [20] suggested that other elements also may replace niobium in the niobium containing intermetallic phases.

#### 4. Conclusions

Microstructure examination revealed that SLM of the alloy Inconel 718 led to the formation of an untypical microstructure. The microstructure features of the SLM material included developed substructure in  $\gamma$  grains and the presence of dispersed precipitates along subgrain boundaries.

The experimental evaluation and calculation of the volume fraction of the niobium containing phases showed that Ti and Mo were not completely presented in the niobium containing phases and were partially dissolved in the matrix  $\gamma$  phase due to rapid cooling and slow diffusion during SLM.

*Acknowledgements. The work was supported by the Program of fundamental researches of Governement Academy of Sciences No. AAAA-A17-117041310215-4.*

## References

1. R. Schafrik, R. Sprague. Key Engineering Materials. 380, 113 (2008).
2. Yi. Huang, T.G. Langdon. Mater. Sci. Eng. A. 410 – 411, 130 (2005).
3. R.P. Jewett, J.A. Halchak. Superalloys 718, 625 and Various Derivatives 1991, 749 (1991).
4. S. Azadian, L.Y. Wei, R. Warren. Materials Characterization. 53, 7 (2004).
5. M.G. Burke, M.K. Miller. Journal de Physique. 50-C8, 395 (1989).
6. J.G. D. Ram, A.V. Reddy, K.P. Rao, G.M. Reddy, J.K. S. Journal of Materials Processing Technology. 167, 73 (2005).
7. W.M. Tuchoa, P. Cuvillier, A. Sjolyst-Kverneland, V. Hansen. Materials Science & Engineering A. 689, 220 (2017).
8. A. Wade, G. Bertali, T. Withaar, D. Foord, B. Freitag, G. Burke. The 16th European Microscopy Congress, Lyon, France. (2016).
9. Y. Huang, T.G. Langdon. Journal of Materials Science. 42, 421 (2007).
10. <http://www.specialmetals.com/assets/smc/documents/alloys/inconel/inconel-alloy-718.pdf>
11. T. Trosch, J. Strößner, R. Völkl, U. Glatzel. Materials Letters. 164, 428 (2016).
12. A. A. Popovich, V. Sh. Sufiarov, I. A. Polozov, E. V. Borisov. Key Engineering Materials. 651 – 653, 665 (2015).
13. S. Raghavan, B. Zhang, P. Wang, C.-N. Sun, M. L. S. Nai, T. Li, J. Wei. Materials and Manufacturing Processes. 32 (14), 1588 (2017).
14. T. Bauer, K. Dawson, A.B. Spierings, K. Wegener. Materials Letters. 164, 428 (2016).
15. A. V. Zavodov, N. V. Petrushin, D. V. Zaitsev. Letters on Materials. 7 (2), 111 (2017). (in Russian) [A. В. Заводов, Н. В. Петрушин, Д. В. Зайцев. Письма о материалах. 7 (2), 111 (2017).] DOI: 10.22226/2410-3535-2017-2-111-116
16. X. Gong, X. Wang, V. Cole, Z. Jones, K. Cooper, K. Chou. Proceedings of the ASME 2015 International Manufacturing Science and Engineering Conference MSEC2015–9317 (2015).
17. E. A. Lukina, K. O. Bazaleeva, N. V. Petrushin, I. A. Treninkov, E. V. Tsvetkova. Metally. 4, 63 (2017). (in Russian) [Е. А. Лукина, К. О. Базалеева, Н. В. Петрушин, И. А. Тренингов, Е. В. Цветкова. Металлы. 4, 63 (2017).]
18. C. Körner. International Materials Reviews. 61 (5), 361 (2016).
19. D.F. Paulonis, J.M. Oblak, D.S. Duvall. ASM-Trans. 62, 611 (1969).
20. M.G. Burke, M.K. Miller. Superalloys 718, 625 and Various Derivatives, 337 (1991).